Front. Phys. 11(4), 117403 (2016)
DOI 10.1007/s11467-016-0554-9

RESEARCH ARTICLE

Impurity scattering effect in Pd-doped superconductor $SrPt_3P$

Kang-Kang Hu[1,2], Bo Gao[2], Qiu-Cheng Ji[2], Yong-Hui Ma[2,3], Hui Zhang[4], Gang Mu[2,†], Fu-Qiang Huang[4], Chuan-Bing Cai[1], Xiao-Ming Xie[2]

[1] *Shanghai Key Laboratory of High Temperature Superconductors, Shanghai University, Shanghai 200444, China*
[2] *State Key Laboratory of Functional Materials for Informatics and Shanghai Center for Superconductivity, Shanghai Institute of Microsystem and Information Technology, Chinese Academy of Sciences, Shanghai 200050, China*
[3] *School of Physical Science and Technology, ShanghaiTech University, Shanghai 201210, China*
[4] *CAS Key Laboratory of Materials for Energy Conversion, Shanghai Institute of Ceramics, Chinese Academy of Sciences, Shanghai 200050, China*
Corresponding author. E-mail: [†] *mugang@mail.sim.ac.cn*

Received December 22, 2015; accepted January 12, 2016

We present a systematic study of the impurity scattering effect induced by Pd dopants in the superconductor $SrPt_3P$. Using a solid-state reaction method, we fabricated the Pd-doped superconductor $Sr(Pt_{1-x}Pd_x)_3P$. We found that the residual resistivity ρ_0 increases quickly with Pd doping, whereas the residual resistance ratio (RRR) displays a dramatic reduction. In addition, both the nonlinear field-dependent behavior of the Hall resistivity ρ_{xy} and the strong temperature dependence of the Hall coefficient R_H at low temperature are suppressed by Pd doping. All the experimental results can be explained by an increase in scattering by impurities induced by doping. Our results suggest that the Pt position is very crucial to the carrier conduction in the present system.

Keywords impurity scattering effect, $SrPt_3P$, superconductors

PACS numbers 74.62.Dh, 74.70.Dd, 74.25.F-

Frontiers of Physics

1 Introduction

The research on high-temperature and unconventional superconductivity has focused recently on materials with transition metal elements because there are strong interplays among the charge, spin, orbital, and lattice degrees of freedom in these systems [1–4]. The discovery of a series of platinum-based superconductors APt_3P (A = Ca, Sr, and La) has recently been reported by the research group of Takayama [5]. These materials have a distorted anti-perovskite structure that resembles the structure of $CePt_3Si$ [6]. Among this family of superconductors, $SrPt_3P$ exhibits the highest T_c of around 8.4 K. After the discovery of $SrPt_3P$, several research groups performed theoretical calculations of the electronic, vibrational, and thermodynamic properties of this material [7–10]. In addition, a series of experiments reportedly revealed the physical properties of $SrPt_3P$. Jawdat *et al.* studied the influence of high pressure and Si doping on the superconductivity of $SrPt_3P$ [11]. Specific heat and inelastic X-ray scattering measurements indicated strong coupling behavior in this material [5, 12], which was in conflict with the electronic structure calculations [10]. Nuclear magnetic resonance investigations indicated a conventional s-wave pairing configuration in this material [13]. Obviously, there still remains sufficient room to further investigate this material. In particular, the calculated densities of states are contributed mainly by the 5*d* states of Pt, which may lead to strong spin–orbital coupling in this system [10, 14]. Therefore, much attention should be paid to the Pt position in the $SrPt_3P$ superconductor.

In this paper, the 4*d* element Pd was successfully substituted at the Pt site of $SrPt_3P$, as revealed by clear changes in the lattice constants. The electron transport in the normal states was studied by resistivity and Hall effect measurements. A clear increase in the residual resistivity ρ_0 and decrease in the residual resistivity ratio (RRR) were observed in the Pd-doped samples, which were attributed to distinct scattering by impurities. This impurity scattering effect also results in suppression of the nonlinear field-dependent behavior of the Hall resistivity ρ_{xy} and strong temperature dependence of the Hall

coefficient R_H in the low-temperature region.

2 Experiments

Samples were prepared through a two-step solid-state reaction. The detailed processes of the sample synthesis were described in our previous paper [14]. The composition of the samples was determined by energy dispersive X-ray spectroscopy measurements on an Oxford Instruments device. The actual doping levels were found to be very close to the nominal composition, so the nominal values of Pd doping will be used in this paper. The structure of the obtained samples was checked using a DX-2700-type powder X-ray diffractometer. The electrical resistance and Hall resistance were measured using a six-probe technique on a physical property measurement system (Quantum Design, PPMS). Magnetic fields of up to 9 T was applied in the direction perpendicular to the sample surface during the Hall effect measurement.

3 Results

3.1 Crystal structure

The crystal structure of this system has been reported by Takayama *et al.* [5]. Here we show the X-ray diffraction (XRD) pattern for one typical sample of this series of materials in Fig. 1. All the main diffraction peaks can be indexed to the structure of $SrPt_3P$. The lattice parameters can be obtained by fitting the XRD data using the software Powder-X [15]. These parameters were determined to be $a = 5.821(2)$ Å and $c = 5.359(6)$ Å, respectively. A comparison with the values for undoped $SrPt_3P$ ($a = 5.809$ Å and $c = 5.383$ Å) indicates that the crystal lattice shows shrinkage along the c axis and expansion along the a axis with increasing doping. This tendency proves that Pd was successfully substituted in the crystal of the present system.

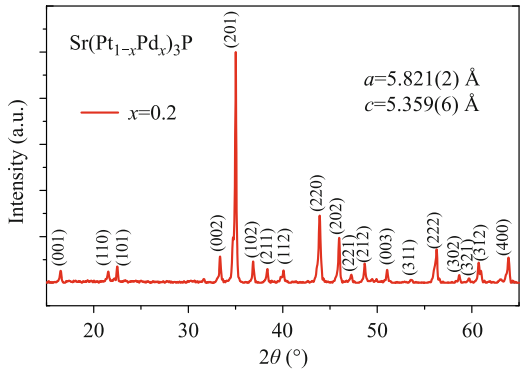

Fig. 1 XRD patterns for one typical $Sr(Pt_{1-x}Pd_x)_3P$ sample with $x = 0.2$.

3.2 Resistivity

We measured the temperature-dependent resistivity of all the samples we synthesized to study the effect of Pd doping on the superconducting properties. The temperature dependence of the resistivity for different doping levels is shown in Fig. 2. All the samples display clear superconducting transitions to zero resistance, which has been discussed in our previous paper [14]. Here, we concentrate on the transport behavior in the normal states. In the normal states above T_c, we observed metallic behavior in the samples with different Pd doping levels. As shown in Fig. 2(a), the conductivity is weakened with increasing Pd content, and the resistivity is enhanced by more than one order of magnitude by Pd doping with $x = 0.4$. This tendency can be represented quantitatively by the residual resistivity ρ_0, which is the resistivity at zero temperature obtained by extrapolating the resistivity data above T_c to 0 K. The doping dependence of ρ_0 is shown in Fig. 3(a). One can see that ρ_0 increases dramatically (up to 59 times) upon Pd doping up to $x = 0.4$. We also show the temperature dependence of the resistivity normalized to 300 K in Fig. 2(b) to investigate the temperature-dependent behavior. The temperature

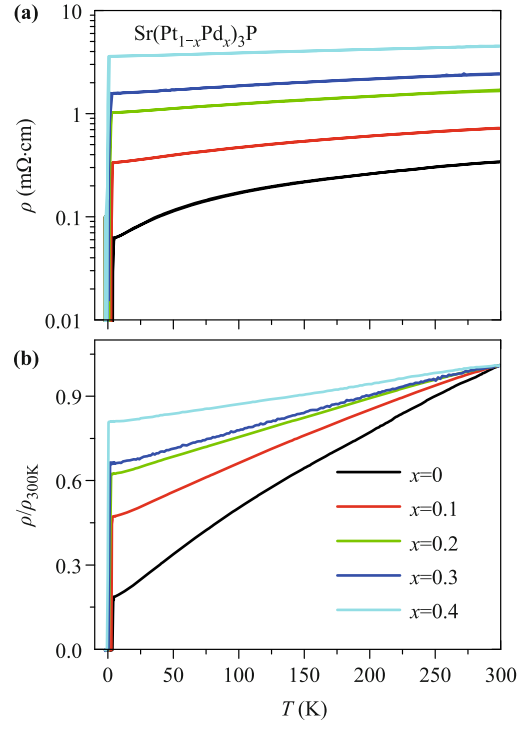

Fig. 2 Temperature dependence of **(a)** logarithmic-scaled and **(b)** normalized resistivity for the samples with $x = 0, 0.1, 0.2, 0.3, 0.4$. Clear superconducting transitions can be seen at low temperatures.

dependent feature was clearly suppressed by Pd doping, indicating a reduction in the residual resistance ratio (RRR = ρ_{300K}/ρ_0), as shown in Fig. 3(b).

Our observations demonstrate a significant increase in the electron scattering by impurities induced by Pd doping. Note that this effect is more remarkable than that in the Si-doped $SrPt_3P_{1-x}Si_x$ system [11], which suggests that the position of Pt is more crucial to the carrier conduction than the P position.

3.3 Hall effect

To obtain further information about the properties of carrier transport and the effects of Pd doping, we measured the Hall effect at various temperatures. Here, we show the results for two $Sr(Pt_{1-x}Pd_x)_3P$ samples with $x = 0$ and $x = 0.2$ for comparison. The field dependence of the Hall resistivity ρ_{xy} of these two samples is shown in Figs. 4(a) and (b), respectively. Here ρ_{xy} was taken as $\rho_{xy} = [\rho(+H) - \rho(-H)]/2$ at each point to eliminate the effect of the misaligned Hall electrodes. The Hall resistivity for both samples is positive, indicating the dominance of hole-type charge carriers in the conduction. In particular, for the undoped sample, the curves show clear nonlinear field-dependent behavior at low temperature, which is a typical feature of the multiband effect. This observation is not novel and is quite consistent with previous experimental results and electronic structure calculations [5, 10, 14]. Upon Pd doping, this nonlinear Hall effect is totally suppressed and linear field-dependent behavior is realized, as revealed by the straight blue line in Fig. 4(b).

The Hall coefficient R_H was determined by the equation

$$R_H = \frac{d\rho_{xy}}{dH}|_{H\to 0}. \quad (1)$$

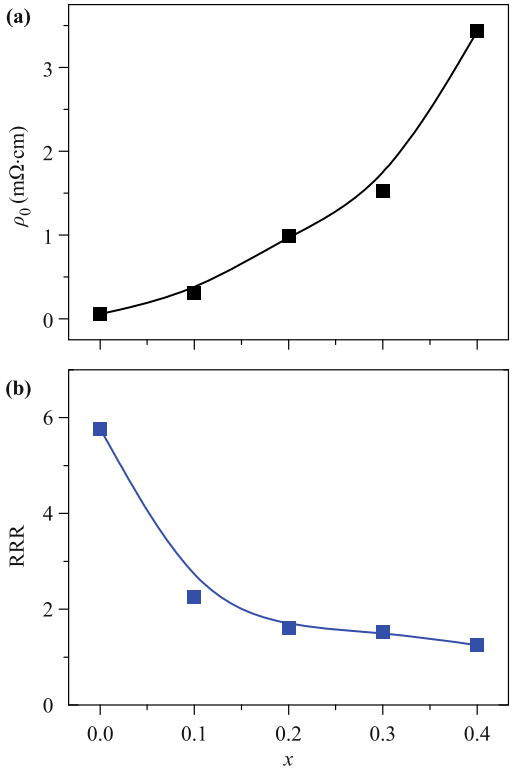

Fig. 3 Doping dependence of **(a)** the residual resistivity (ρ_0) and **(b)** the residual resistance ratio (RRR).

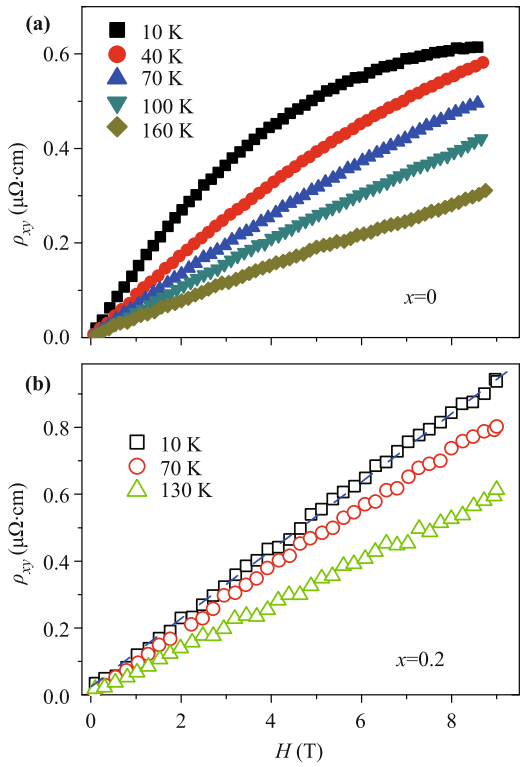

Fig. 4 Field dependence of the Hall resistivity ρ_{xy} at different temperatures for the $Sr(Pt_{1-x}Pd_x)_3P$ samples with **(a)** $x = 0$ and **(b)** $x = 0.2$. The straight blue line is a guide for the eyes.

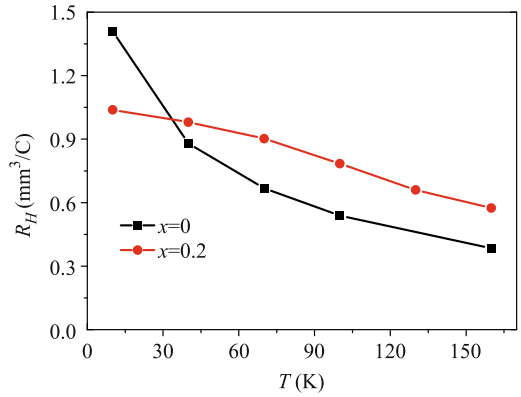

Fig. 5 Temperature dependence of the Hall coefficient R_H for the two samples with $x = 0$ and 0.2.

The temperature dependence of R_H for the two samples with $x = 0$ and $x = 0.2$ is shown in Fig. 5. The variation of R_H at different temperatures for $SrPt_3P$ is clearly larger than that for $Sr(Pt_{0.8}Pd_{0.2})_3P$. For a simple two-band scenario with different types of carriers, the Hall coefficient R_H in the low-field limit can be expressed as [16]

$$R_H = \frac{1}{e}\frac{n_h\mu_h^2 - n_e\mu_e^2}{(n_h\mu_h + n_e\mu_e)^2}, \quad (2)$$

where n_i and μ_i $(i = h, e)$ are the charge density and the mobility of the hole and electron band, respectively. Unlike the case for the single-band system, where the Hall coefficient is determined only by the charge density, the mobility should also be considered in this multiband case. The mobility is known to be proportional to the scattering time τ. Typically the scattering time τ has a strong temperature dependence, which leads to the strong temperature dependence of R_H, as has been observed in other multiband systems [17–21]. In contrast, R_H normally shows a weak temperature dependence in a conventional single-band system. Our result here is consistent with the suppression of the nonlinear field dependence of ρ_{xy} represented in the above paragraph.

The first-principles calculations in our previous work [14] suggest that Pd doping does not suppress the multiband features of the electronic structure. Consequently, the suppression of the nonlinear field dependence of ρ_{xy} and the weakening of the temperature dependence of R_H are hard to attribute to the changes in the band structure. We checked the change in the scattering time after Pd doping and found that it is responsible for the observed behavior of the Hall effect. In a solid, electrons can scatter from phonons and impurities, and the total scattering rate can be expressed as [16]

$$1/\tau = 1/\tau_{ph} + 1/\tau_{imp}, \quad (3)$$

where τ_{ph} and τ_{imp} are the scattering time from phonons and impurities, respectively. It is well known that τ_{imp} is temperature-independent and determines the residual resistivity ρ_0. As shown in Fig. 3(a), ρ_0 increases dramatically with Pd doping, which means that the scattering rate from impurities $(1/\tau_{imp})$ increases rapidly. Apparently, the increase in this T-independent term in Eq. (3) will weaken the temperature dependence of the total scattering rate $1/\tau$ and the Hall coefficient R_H accordingly.

4 Conclusion

In conclusion, we successfully substituted Pd into the Pt position in the superconductor $SrPt_3P$. Pd doping changes the lattice parameters and transport properties. Both the conductivity and the residual resistance ratio are dramatically suppressed by Pd doping. The multiband features, as revealed by the nonlinear field dependence of ρ_{xy} and the strong temperature dependence of R_H, are also suppressed by doping. All the experimental facts can be interpreted in terms of doping-induced enhancement of scattering from impurities. Our results reveal the importance of Pt in the electron transport performance, to which more attention should be paid in order to understand the superconducting mechanism of the present system.

Acknowledgements This work was supported by the National Natural Science Foundation of China (Grant No. 11204338), the "Strategic Priority Research Program (B)" of the Chinese Academy of Sciences (Grant No. XDB04040300), and the Youth Innovation Promotion Association of the Chinese Academy of Sciences (Grant No. 2015187). This work was partly sponsored by the Science and Technology Commission of Shanghai Municipality (Grant Nos. 14DZ2260700 and 14521102800).

References

1. J. G. Bednorz and K. A. Müller, Possible high T_c superconductivity in the Ba-La-Cu-O system, *Z. Phys. B: Condens. Matter* 64(2), 189 (1986)
2. Y. Kamihara, T. Watanabe, M. Hirano, and H. Hosono, Iron-based layered superconductor $La[O_{1-x}F_x]FeAs$ (x = 0.05–0.12) with T_c = 26 K, *J. Am. Chem. Soc.* 130(11), 3296 (2008)
3. W. Li, C. Setty, X. H. Chen, and J. P. Hu, Electronic and magnetic structures of chain structured iron selenide compounds, *Front. Phys.* 9(4), 465 (2014)
4. G. Mu, V. Sandu, W. Li, and B. Shen, Exotic superconductivity in correlated electron systems, *Adv. Condens. Matter Phys.* 2015, 180195 (2015)
5. T. Takayama, K. Kuwano, D. Hirai, Y. Katsura, A. Yamamoto, and H. Takagi, Strong coupling superconductivity at 8.4 K in an antiperovskite phosphide $SrPt_3P$, *Phys. Rev. Lett.* 108(23), 237001 (2012)
6. E. Bauer, G. Hilscher, H. Michor, Ch. Paul, E. W. Scheidt, A. Gribanov, Yu. Seropegin, H. Noel, M. Sigrist, and P. Rogl, Heavy fermion superconductivity and magnetic order in noncentrosymmetric $CePt_3Si$, *Phys. Rev. Lett.* 92(2), 027003 (2004)
7. C. J. Kang, K. H. Ahn, K. W. Lee, and B. I. Min, Electron and phonon band-structure calculations for the antipolar $SrPt_3P$ antiperovskite superconductor: Evidence of low-energy two-dimensional phonons, *J. Phys. Soc. Jpn.* 82(5), 053703 (2013)
8. H. Chen, X. F. Xu, C. Cao, and J. H. Dai, First-principles calculations of the electronic and phonon properties of

APt_3P (A = Ca, Sr, and La): Evidence for a charge-density-wave instability and a soft phonon, *Phys. Rev. B* 86(12), 125116 (2012)

9. R. Szczęśniak, A. P. Durajski, and L. Herok, Theoretical description of the $SrPt_3P$ superconductor in the strong-coupling limit, *Phys. Scr.* 89(12), 125701 (2014)
10. I. A. Nekrasov and M. V. Sadovskii, Electronic structure of new multiple band Pt-pnictide superconductors APt_3P, *JETP Lett.* 96(4), 227 (2012)
11. B. I. Jawdat, B. Lv, X. Zhu, Y. Xue, and C. Chu, High-pressure and doping studies of the superconducting antiperovskite $SrPt_3P$, *Phys. Rev. B* 91(9), 094514 (2015)
12. D. A. Zocco, S. Krannich, R. Heid, K. P. Bohnen, T. Wolf, T. Forrest, A. Bossak, and F. Weber, Lattice dynamical properties of superconducting $SrPt_3P$ studied via inelastic X-ray scattering and density functional perturbation theory, arXiv: 1510.02012 (2015)
13. T. Shiroka, M. Pikulski, N. D. Zhigadlo, B. Batlogg, J. Mesot, and H. R. Ott, Pairing of weakly correlated electrons in the platinum-based centrosymmetric superconductor $SrPt_3P$, *Phys. Rev. B* 91(24), 245143 (2015)
14. K. K. Hu, B. Gao, Q. C. Ji, Y. H. Ma, W. Li, X. G. Xu, H. Zhang, G. Mu, F. Q. Huang, C. B. Cai, X. M. Xie, and M. H. Jiang, The effects of electron correlation and spin-orbit coupling in the isovalent Pd-doped superconductor $SrPt_3P$, arXiv: 1601.02782 (2015)
15. C. Dong, PowderX: Windows-95-based program for powder X-ray diffraction data processing, *J. Appl. Cryst.* 32(4), 838 (1999)
16. J. Singleton, Band Theory and Electronic Properties of Solids, Oxford: Oxford University Press, 2001
17. G. Mu, B. Zeng, X. Zhu, F. Han, P. Cheng, B. Shen, and H. H. Wen, Synthesis, structural, and transport properties of the hole-doped superconductor $Pr_{1-x}Sr_xFeAsO$, *Phys. Rev. B* 79(10), 104501 (2009)
18. G. Mu, B. Zeng, P. Cheng, X. Zhu, F. Han, B. Shen, and H. H. Wen, Superconductivity at 15.6 K in calcium-doped $Tb_{1-x}Ca_xFeAsO$: The structure requirement for achieving superconductivity in the hole-doped 1111 phase, *Europhys. Lett.* 89(2), 27002 (2010)
19. H. Yang, Y. Liu, C. Zhuang, J. Shi, Y. Yao, S. Massidda, M. Monni, Y. Jia, X. Xi, Q. Li, Z. K. Liu, Q. Feng, and H. H. Wen, Fully band-resolved scattering rate in MgB_2 revealed by the nonlinear hall effect and magnetoresistance measurements, *Phys. Rev. Lett.* 101(6), 067001 (2008)
20. G. Mu, H. Yang, and H. H. Wen, Multiband effect in the noncentrosymmetric superconductors $Mg_{12-\delta}Ir_{19}B_{16}$ revealed by Hall effect and magnetoresistance measurements, *Phys. Rev. B* 82(5), 052501 (2010)
21. L. Fang, H. Luo, P. Cheng, Z. Wang, Y. Jia, G. Mu, B. Shen, I. I. Mazin, L. Shan, C. Ren, and H. H. Wen, Roles of multiband effects and electron-hole asymmetry in the superconductivity and normal-state properties of $Ba(Fe_{1-x}Co_x)_2As_2$, *Phys. Rev. B* 80, 140508(R) (2009)